Transactions of the **14th International Conference on Structural Mechanics in Reactor Technology** (SMiRT 14), Lyon, France, August 17-22, 1997

B03/1

Computational aspects of hybrid micromechanical / continuum modeling of deformation

Sauvé R.G., Badie N.
Ontario Hydro Technologies, Canada

ABSTRACT

This paper describes the implementation of a time-dependent constitutive model for an anisotropic material into a three dimensional finite element scheme. The model departs from the usual continuum approach in that the material behaviour is based on a polycrystalline idealization. A hybrid continuum/microstructural solution procedure for large three dimensional problems is described along with applications to flaw assessment in nuclear power plant components.

INTRODUCTION

The need for greater accuracy in the prediction of stress redistribution near flaws due to creep in nuclear power reactors has been one of the motivating factors in the development of micromechanical material models [1,2]. These are considered accurate alternatives to semi-empirical continuum models. Micromechanical models have the advantage of providing a higher level of detail for anisotropic materials in localized areas of high stress, such as the flaw shown in figure 1. These models can account for the evolution of intergranular constraints, microstructure and texture with time. This is in contrast to continuum models of anisotropy such as Hill's ellipsoid [5] where the effects of anisotropy are characterized by constant coefficients. However, the use of micromechanical models in determining the response of three dimensional solids under various far field loading conditions can become computationally intractable unless special strategies are adopted.

The usual approach in the characterization of materials for the subdomains of the finite element method is a continuum model of elastoplasticity, creep and growth with closed form equations. Alternatively, self-consistent polycrystalline models of grain interaction [1,2], which couple the response of each grain to the overall response and average properties of the material, generally involve iterative procedures. Such an accurate account of anisotropy is essential in applications involving irradiation creep and growth and thermal creep under large deformation.

In order to treat the anisotropic behaviour of power reactor materials, such as Zr-2.5Nb, polycrystal models are being implemented into a three dimensional nonlinear finite element code currently used in simulating the response of in-reactor components. The resulting hybrid code combines the continuum model with the micromechanical material models. An important issue in the implementation of microstructural material models into finite element software is the development of strategies to reduce the large memory requirements and increased operations associated with polycrystal calculations.

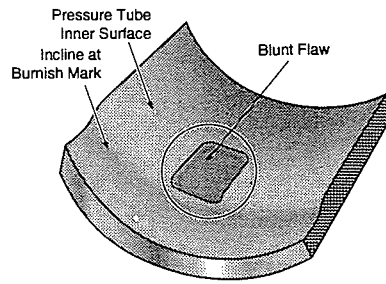

Figure 1: Schematic of Pressure Tube Fret Flaw

In this paper, the implementation of a self-consistent polycrystalline strain rate model, described in [1,2], into an existing three dimensional continuum finite element code for finite deformation [11] is described. The focus is on the computational aspects of the implementation such as the dynamic relaxation solution procedure for creep [9,10], the use of interpolation tables [3,4] to avoid time consuming polycrystal calculations and the use of three dimensional elements [8] that are efficient yet accurate for this class of problem. Examples such as an assessment of notch tip stress relaxation for a flaw geometry, are presented along with comparisons of predictions with experiment.

CREEP CONSTITUTIVE MODELLING

In general, a constitutive law for high stress thermal creep may relate the strain rate at a given point in a material to some material properties, to the conditions imposed on the material, and to accumulated creep strain. This can be represented as follows;

$$\dot{\varepsilon}_c^{\tau} = f\,(\varepsilon_c^{\tau},\ T,\ \sigma^{\tau},\ M_p) \tag{1}$$

where $\dot{\varepsilon}_c^{\tau}$ is the creep strain rate tensor, τ is time, ε_c^{τ} is the accumulated creep strain tensor, T is temperature, σ^{τ} is the stress tensor and M_p is a set of material properties. An approach similar to that used in describing plastic deformation, where component stresses and strains are derived from effective stress and effective strain is general practice in continuum modelling. The effective stress $\bar{\sigma}$ is calculated according to Hill's adaptation [5] of the von Mises yield criterion for anisotropic materials. Thus, in the general case, we have;

$$\bar{\sigma} = \left[F\left(\sigma_{11} - \sigma_{22}\right)^2 + G\left(\sigma_{22} - \sigma_{33}\right)^2 + H\left(\sigma_{33} - \sigma_{11}\right)^2 + 2L\sigma_{12}^2 + 2M\sigma_{23}^2 + 2N\sigma_{31}^2\right]^{1/2} \tag{2}$$

where σ_{ij} are the components of true (Cauchy) stress, and F,G,H,L,M,N are constant coefficients of anisotropy. In the case of a cylindrical shell, the indices *1, 2* and *3* represent the axial (a), hoop (t) and radial (r) directions respectively.

The drawbacks of this approach are: i) the difficulty of producing realistic predictions outside the range of the variables used to fit the law to experiments and ii) the absence of a physical basis for the evolution of anisotropy during deformation (e.g. constant values of F, G, H...).

Anisotropy and Interpolation Table Technique

These concerns have led to the development of alternative methods based on solid state material modelling [1,2] in which the material is regarded as an aggregate of crystal orientations whose response is averaged over the constituent grains. The advantage of such an approach is that the response is based on deformation mechanisms acting at the grain level. In this way the material anisotropy enters the model through the texture of the aggregate as the material deforms. The disadvantages of this approach are: i) experiments are required to characterize the single crystal properties that enter into the formulation and their evolution with strain, ii) the direct use of polycrystal codes for describing the constitutive response in numerical schemes, such as the implementation described in [1] for steady state creep, can be prohibitively expensive for high stress creep and iii) it is difficult to introduce the evolution of single crystal mechanisms from first principles.

In order to address point (ii) above, a method has been proposed [3,4] that combines the advantages of both continuum/empirical and polycrystal approaches to provide an efficient and accurate prediction of creep response. The polycrystal model describes the anisotropy of the high stress creep response, while the empirical equation is used to describe the strain dependence of the creep rate in the transient regime. Efficiency is achieved by creating a lookup table that contains creep rates associated with a complete sampling of the stress space and interpolating between them for an arbitrary combination of stress components.

For flaw assessments of nuclear pressure tube components this model contains some macroscopic and microscopic parameters which are empirically fit to tensile experiments along the axial and hoop directions. The anisotropy is accounted for by means of the interpolation table, which in turn is generated by running a polycrystal code for a large number of stress states. The creep model calculates the thermal creep rate induced by a general stress tensor imposed upon a material whose properties are the ones of a pressure tube. Details are given in [3,4]. The form of the law is:

$$\dot{\varepsilon}_c = f(\varepsilon_c^{ef}, T, \sigma^{ef})\, \dot{\varepsilon}^{IT}(\sigma) \qquad (3)$$

where $\dot{\varepsilon}^{IT}$ is the response in tensor form of the material from the interpolation table for a stress tensor σ. This assumes that the response to an imposed stress, σ, is proportional to the response that the polycrystal predicts. The implicit assumption is that the ratio of the creep components is always the same for a given stress direction independent of the accumulated creep strain or temperature. Two anisotropies are accounted for by the interpolation table; one associated with the ratio of the components of the creep strain rate tensor for a given stress and one due to the difference in the components associated with the same stress applied in different directions (e.g. stress applied in *11* or *22* directions lead to two different $\dot{\varepsilon}^{IT}$).

The scalar $f\ (\varepsilon_c^{\,ef}, T, \sigma^{ef})$ is intended to scale the creep strain rate for strain hardening, temperature. Since this scalar does not describe the anisotropy of creep, care must be taken when using the empirical data for a particular material, to ensure that the responses for the particular reference direction chosen reproduce the tensile tests for this direction.

COROTATIONAL DESCRIPTION FOR LOCAL MATERIAL AXES

In order to account for an arbitrary orientation of material axes consistent with an anisotropic material that rotates with a deforming three dimensional body, an algorithm has been implemented into the three dimensional nonlinear continuum element formulation described in [8]. The key feature of this option is the ability to track the orientation of the material axes (and constitutive properties) for finite deformation. This requires an incremental orthogonal tensor transformation of a rotation tensor. The initial orientation of the material axes is specified for each element in the model, along the axial, hoop and radial directions as shown in figure 2.

During the solution, the constitutive calculations that include elastic orthotropy, plasticity and calls to the micromechanical creep model, are performed on an updated corotational material axes that rotates with the element. The integration of the material quantities are performed and referenced on this frame. Thus, all stress values are Cauchy stresses and are related to their log strain conjugates which are reported as output on their terminal frame. A brief summary of the algorithm is given in the following section.

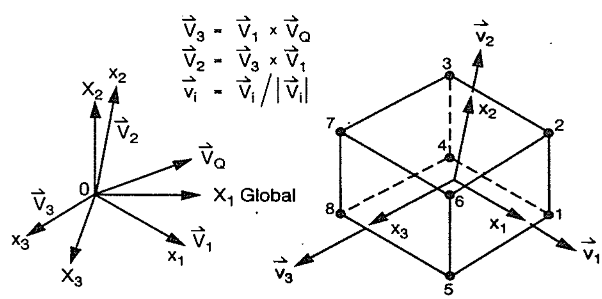

Figure 2: Local Element Material Axes System

Implementation of the Local Material Axes Algorithm

In the continuum based finite element code, the kinematic quantities available for the constitutive calculations at each material time τ (as opposed to each iteration cycle t) for each element of the model are velocity strain or rate of deformation tensor, D, in the global reference system, the spin tensor or skew symmetric part, W, of the velocity gradient, L, also referred to the global system, and the current accumulated plastic and creep strains ε_p and ε_c at cycle t. The velocity gradient, L, is defined in terms of the current configuration x_i as;

$$L = \frac{\partial \dot{x}}{\partial x} = D + W \tag{4}$$

The approach adopted treats the constitutive law in the local axis of anisotropy at the current time by rotating D into the local material frame and performing the constitutive calculations such as creep strain updates and stress integration in the specified local axes system. The key to the application of the algorithm to finite deformation is the accurate integration of a spinning rotation tensor, R, and maintaining its orthogonality. The spin tensor, W, is considered for the hybrid anisotropic material calculations since it represents the average rate of rigid rotation of the material during large deformation. Other spin tensors have been considered in the finite deformation of continua [6,7], but here, the average rotation is used for the corotational frame while local material rotations are accounted for by the grain interaction of the polycrystalline model.

The algorithm is summarized in the following steps;

i) Form an initial rotation tensor, R, relating the axis of anisotropy to the reference axis, for each material (i.e. element) point using the direction cosines specified as shown in figure 2.

ii) Update the rotation tensor R at each iteration cycle $t + \Delta t$ and material creep time τ using an incremental rotation tensor ΔR following the method in [6] as;

$$R^{t+\Delta t} = \Delta R R^{t} = [I - \Delta t W/2]^{-1} [I + \Delta t W/2] R^{t} \tag{5}$$

iii) Obtain values of velocity strain, d, in the local material axes;

$$d^{t+\Delta t/2} = (R^{T})^{t+\Delta t} D^{t+\Delta t/2} R^{t+\Delta t} \tag{6}$$

iv) Perform constitutive calculations for the local stress increment $\Delta\sigma'$ in the local material axes using elastic orthotropic properties, current anisotropic creep strain rates and plastic strains represented by the functional C as;

$$\Delta\sigma'^{t+\Delta t} = C(\Delta t d^{t+\Delta t/2}, (\Delta\varepsilon_c^{\tau})^{t+\Delta t}, (\Delta\varepsilon_c^{\tau})^{t}, \Delta\varepsilon_p^{t+\Delta t}) \tag{7}$$

v) Update stresses in local system;

$$\sigma'^{t+\Delta t} = \sigma'^{t} + \Delta\sigma'^{t+\Delta t} \tag{8}$$

vi) Rotate stresses into global reference axes;

$$\sigma^{t+\Delta t} = R^{t+\Delta t} \sigma'^{t+\Delta t} (R^{T})^{t+\Delta t} \tag{9}$$

vii) Evaluate internal element force vector F_{int}, assemble contribution to system internal force vector and repeat the solution for equations of equilibrium at iteration cycle $t + \Delta t$.

Once convergence for a specific load level and creep time is obtained, the new load and creep time are applied and the steps repeated until the final creep time is attained. The axis of anisotropy defines both the elastic and creep properties. The algorithm provides an approach that ensures a proper rotating material frame during finite deformation.

DYNAMIC RELAXATION SOLUTION

Traditionally, the finite element method has been applied to steady state problems using implicit methods, where large numbers of equations are formed and solved using direct solvers such as frontal, skyline or Cholesky-type methods. When non-linearities exist, equilibrium iterations must be performed using Newton-Raphson or quasi-Newton techniques at each load level. In the presence of complex geometry and non-linear material behaviour solutions using implicit methods often become intractable. In [9] an iterative solution technique known as dynamic relaxation (DR) is described that avoids the use of direct solvers.

The explicit nature of dynamic relaxation makes it especially attractive in computational mechanics since all quantities are treated as vectors and the large storage requirements associated with large matrices are avoided. In addition, the computational effort increases only proportionally to the number of degrees of freedom so that large scale problems involving hundreds of thousands of degrees of freedom are possible (i.e. there are no bandwidth limitations). The simple logic of the procedure permits an elegant algorithmic structure providing a convenient framework for the treatment of non-linearities. In addition, equilibrium is tested directly on the current configuration considering the Cauchy (i.e. true) stress acting on the body. The underlying idea behind DR is to derive problem dependent, adaptive critical damping, mass and time step that attenuate the transient response leaving the steady state solution for an applied loading. Many previous works using DR allow overshoot of the solution. While this is not a severe limitation for problems which are strictly elastic in nature, this is clearly not acceptable for non-linear problems such as those involving hysteretic elastic-plastic materials, creep and contact problems where responses are history dependent. The algorithm for DR [9] considered in this work for the solution of time-dependent deformation problems ensures that the steady state solution is devoid of overshoot.

Inclusion of Creep in Dynamic Relaxation

Neglecting body forces, the discretized equations of motion for the system are as follows;

$$M \frac{d\dot{x}}{dt} + F_{int}^{t} = F_{ext}^{t} \tag{10}$$

where;

M = scaled mass matrix

F_{int}^{t} = internal force vector $= \sum_{k=1}^{NE} \left[\int_{V_k} B^T \sigma \, dV \right]$

F_{ext}^{t} = external traction forces

NE = number of elements

B^T = element matrix relating velocity strain to velocity at node degrees of freedom.

The relevant boundary conditions are applied to the system of discretized equations and a solution is obtained in terms of velocities and displacements. In the analysis of creep deformation, the response of the system is dependent both on external loading and the strain time history. In general, this deformation is governed by a creep law which relates the creep strain rate tensor, $\dot{\varepsilon}_c$, in terms of stress, σ, accumulated creep strain, ε_c, and temperature, T. The use of DR in steady state creep has been previously described [10]. Unlike the work in [10], the material anisotropy is

Although this method is only conditionally stable, its simplicity in implementation and the use of controlled time steps have made it particularly effective in this application. Once the current stress $\sigma^{t+\Delta t}$ is known, the internal force vector is obtained at the next cycle;

$$F_{int}^{t+\Delta t} = \sum_{k=1}^{NE} \left[\int_{V_k} \left(B^{\,t}\right)^T \sigma^{t+\Delta t} \, dV \right] \tag{17}$$

Upon convergence, the stresses and strains are then used as initial conditions for the next creep time step, $\tau + \Delta\tau$. The overall solution procedure is shown in figure 3.

APPLICATIONS

The aforementioned technique has been implemented as an additional material module into a nonlinear three dimensional finite element code used for finite deformation [11]. This section describes a benchmark case and an application to an in-reactor pressure tube flaw assessment. In all cases, three dimensional nonlinear isoparametric element technology with single point quadrature [8] is used in conjunction with previously described methods. The material is Zr-2.5Nb with the material textures obtained from [3,4]. The convention for labelling the pressure tube axes in the cases described and for referring the tensor components is as follows: *1* = axial direction, *2* = transverse (hoop) direction, and *3* = radial direction. All computer runs were conducted on a HP-C180 workstation using the Unix operating system.

Smooth Specimen Tensile Creep Experiment

In [12] high stress creep tensile experiments were conducted on smooth specimens of Zr-2.5Nb nuclear pressure tube material for a range of stress in the axial and hoop directions. The advantage of the test data described in [12] is the detail regarding the primary creep. In order to provide a suitable benchmark of the proposed numerical hybrid implementation for creep described in the previous sections, simulations of a number of these tests were carried out. These simulations provide a suitable assessment of the hybrid creep formulation since they are completely independent of the tests [3] used to derive the scalar component of the creep law in equation 3. The measured texture of a similar Zr-2.5Nb tube material was used to generate discrete texture data containing 144 orientations. This is used along with single crystal properties in polycrystal calculations to generate the interpolation table [4] to account for anisotropy.

The geometry of the test specimen is shown in figure 4a. The finite element model consists of 1350 three dimensional elements and 1820 nodes defining the topology of a 1/8 model of the test specimen. Four tests were selected from [12] as indicated in figure 4a. Each of the pair of tests CSCT10/14 and CSCT17/28 were conducted at 250°C in the material transverse direction.

The magnitudes of stress for each set of tests were 500 MPa and 455 MPa corresponding to 89% and 81% respectively, of the initial yield stress in the hoop direction. The material/experimental variability observed in the tests are apparent in figures 4a and 4b. A comparison of the these experimental results with predictions of hoop creep strain, ε_{c22}, using the technique described herein is shown in figures 4a and 4b.

accounted for using the interpolation table $\dot{\varepsilon}_c^{IT}$, based on a polycrystalline model.

It is assumed that an increment in creep strain can be obtained from the rate form of the creep law given by equation (3). The effect of creep on the solution is introduced at the element level where the constitutive calculations are performed. It should be noted that time t represents a cycle in the solution of a creep time step, τ. That is, within each creep time increment, dynamic relaxation is used to obtain a converged steady state solution. The next creep time increment is imposed and the DR process is repeated. For a given stress state at a solution cycle $t+\Delta t$ the increment in total strain, $\Delta\varepsilon$, is given as the sum of the elastic, $\Delta\varepsilon_e$, and creep, $\Delta\varepsilon_c$, strain increments. While time-independent plasticity can be considered, it is assumed negligible in the present description of material creep behaviour.

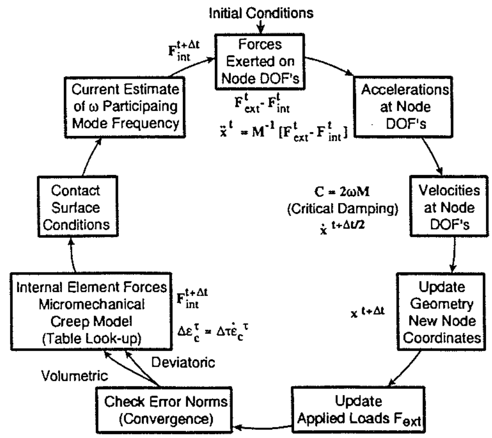

Figure 3: Nonlinear Computational Cycle - Dynamic Relaxation

The following basic steps are performed at each cycle of the iterative solution:

i) obtain the total strain,

$$\Delta\varepsilon^{t+\Delta t} = \Delta\varepsilon_e^{t+\Delta t} + \Delta\varepsilon_c^{t+\Delta t} = D^{t+\Delta t/2} = \Delta t B\, {}^t\dot{x}^{t+\Delta t/2} \tag{11}$$

ii) calculate elastic strain increment using current change in creep strain increment from polycrystalline interpolation table,

$$\Delta\varepsilon_e^{t+\Delta t} = \Delta\varepsilon^{t+\Delta t} - \Delta\varepsilon_c^{t+\Delta t} + \Delta\varepsilon_c^{t} \tag{12}$$

iii) recover stress increment $\Delta\sigma$ using orthotropic elastic constitutive relation,

$$\Delta\sigma = C\,(\Delta\varepsilon_e^{t+\Delta t}) \tag{13}$$

iv) update current stress at cycle $t+\Delta t$

$$\sigma^{t+\Delta t} = \sigma^t + \Delta\sigma \tag{14}$$

v) update creep strain at cycle t

$$\varepsilon_c^{t+\Delta t} = \varepsilon_c^{t} + \Delta\varepsilon_c^{t+\Delta t} \tag{15}$$

A creep strain increment $\Delta\varepsilon_c$ is defined in time interval $\Delta\tau$ using an Euler time stepping scheme:

$$\Delta\varepsilon_c = \dot{\varepsilon}_c^{\tau}\,\Delta\tau \tag{16}$$

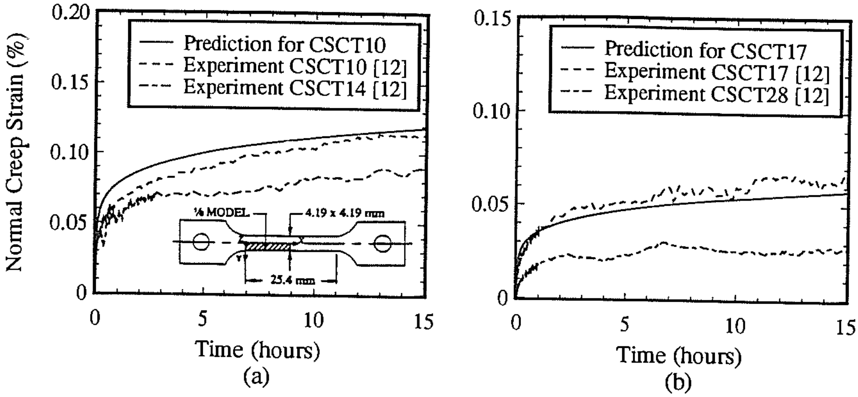

Figure 4: Evolution of Transverse Creep Strain
Simulation of Tensile Creep Experiments [12] on Zr-2.5Nb

Excellent agreement is observed as the predictions are consistent with experimental results even in light of the obvious variability in the physical measurements. Of particular interest is the good agreement in the primary stage of creep. It should be noted that this set of tests were carried out independently of those used in fitting the polycrystal model.

Pressure Tube Flaw Creep

In this application, the simulation of creep in a pre-irradiated Zr-2.5Nb pressure tube containing a fret flaw, similar to that shown schematically in figure 1, is considered. The prediction was carried out at a temperature of 250 °C. In this case a combination of creep and stress relaxation is introduced due to the localization of stress around the flaw. The geometry of the flaw necessitates the use of a refined three dimensional model.

The three dimensional finite element mesh, shown in figure 5, consists of 15488 element and 18012 nodes. Use of symmetry permits a detailed finite element model representing a quarter of the flawed pressure tube. Nominal tube parameters are internal radius of 52 mm and thickness of 4 mm. The partial model in figure 5 indicates the high mesh refinement in the region of the fret flaw. It is clear from the mesh and its large associated bandwidth that the proposed explicit steady state solution has distinct advantages over its implicit counterpart.

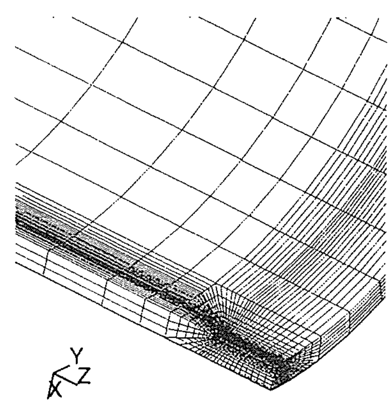

Figure 5: Pressure Tube Finite Element Model

As before, the interpolation table for this material was generated for the measured texture of a pressure tube using polycrystal calculations [4]. An internal pressure of 15.5 MPa is applied to the tube and results in a nominal far field hoop stress of 202 MPa. The maximum local stress, σ_{22}, prior to creep, is 707 MPa which is located in the root region of the flaw.

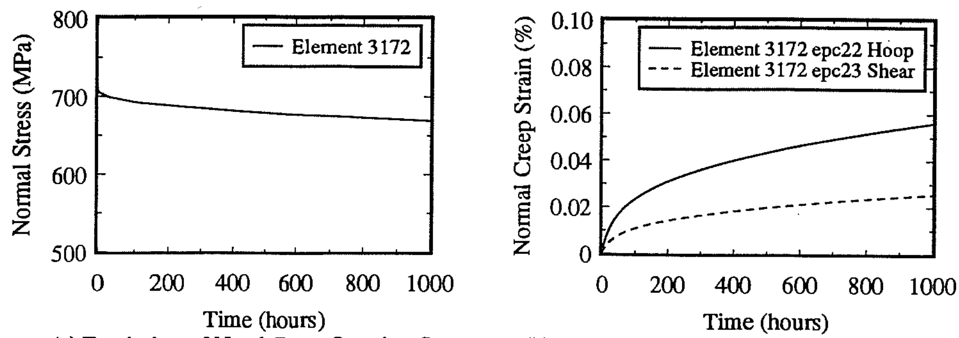

(a) Evolution of Notch Root Opening Stress (b) Evolution of Notch Root Opening Creep Strain

Figure 6: Creep Simulation of Pressure Tube with Fret Flaw

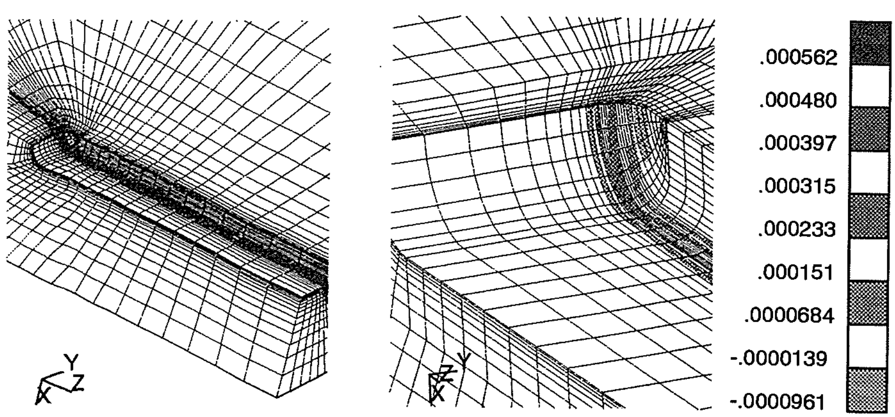

(a) (b)

Figure 7: Pressure Tube Flaw - Hoop Strain, ε_{c22}, Distribution at 1000 hours

The evolution of local stress, σ_{22}, and creep strains, ε_{c22} , ε_{c23}, during over 1000 hours are shown in figures 6a and 6b respectively. Detailed contour plots of the flawed region indicating the distribution of creep strain, ε_{c22}, after 1000 hours of creep are shown in figures 7a (remote view) and 7b (closeup view). The corresponding plots for stress, σ_{22}, are shown in figures 8a and 8b. The figures show that the dominant response occurs in the sharp regions of the fret flaw as expected.

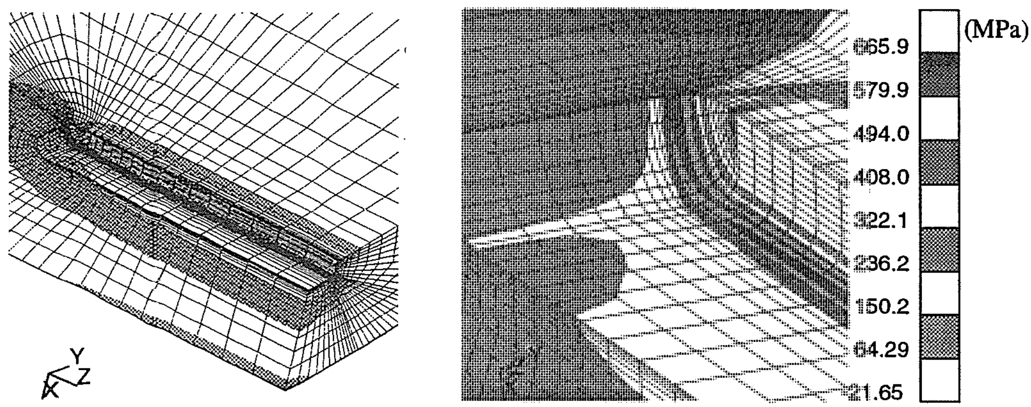

(a) (b)

Figure 8: Pressure Tube Flaw - Local Hoop Stress, σ_{22}, Distribution at 1000 hours

CONCLUSIONS

A numerical procedure that effectively combines a continuum approach using three dimensional finite element techniques with micromechanical material characterization of anisotropic creep, using a polycrystalline interaction model has been presented. This hybrid solution concept has been applied to the prediction of stress redistribution in large scale flaw models. Tractable solutions for problems involving hundreds of thousands of degrees of freedom are feasible on relatively low cost workstations. Current work is underway on similar approaches for large deformation anisotropic plasticity and irradiation creep. This proposed hybrid approach shows promise and should lead to significant improvement in the way materials at discontinuities are modelled in the future.

ACKNOWLEDGEMENTS

The work described in this paper was funded by the CANDU Owner's Group (COG) research program. The authors wish to acknowledge C.Tomé of Los Alamos National Laboratory formerly of Whiteshell Research Laboratory and N.Christodoulou of Atomic Energy of Canada Chalk River Laboratory for the development of the polycrystalline creep models and discussions related to the numerical implementation of the micromechanical material models. Thanks are also due to E. Ho of Ontario Hydro Technologies and R. Klassen of Atomic Energy of Canada Chalk River Laboratory for providing experimental data.

REFERENCES

1. Christodoulou, N. et al, *Modelling In-Reactor deformation of Zr-2.5Nb Pressure Tubes in CANDU Power Reactors*, Proceedings of the 11th Symposium: Zirconium in the Nuclear Industry, American Society for Testing and Materials, Garmisch-Partenkirchen, 1995.
2. Tomé, C., So, C., Woo, C., Self-Consistent *Calculation of Steady State Creep and Growth in Textured Zirconium,* Philosophical Magazine A, 67, 1993.
3. Tomé, C., Christodoulou, N., Klassen, R., *Thermal Creep Equation for Stress Relaxation at Flaws: Report on Version 2,* Atomic Energy of Canada Report No. RC-1539, June 1996.
4. Lhuillier, D., Tomé, C., *Modeling of Irradiation and Thermal Creep of Pressures Tubes II - Polycrystal Description of Thermal Creep by Means of an Interpolation Table*, Atomic Energy of Canada Report No. RC-1223, June 1996.
5. Hill, R., *The Mathematical Theory of Plasticity*, Oxford Press, 1950.
6. Dubey, R.N., Sauvé, R.G., *Numerical Integration of Rate Constitutive Equations Under Finite Deformation*, Journal of Nuclear Engineering and Design, 135, 1992.
7. Johnson, G., Bammann, D., *A Discussion of Stress Rates in Finite Deformation Problems*, International Journal of Solids and Structures, 20, No. 8, 1984.
8. Metzger, D.R., Sauvé, R.G., *Three-Dimensional Hourglass Stabilization for One Point Quadrature Finite Elements*, in Design Analysis, Robust Methods and Stress Classification, ASME PVP, 265, 1993.
9. Sauvé, R.G., Metzger, D.R., *Advances in Dynamic Relaxation Techniques for Nonlinear Finite Element Analysis*, Journal of Pressure Vessel Technology, ASME Trans., 117, 1995.
10. Sauvé, R.G., Badie, N., *Nonlinear Shell Formulation for Reactor Fuel Channel Creep*, in Design Analysis, Robust Methods and Stress Classification, ASME PVP, 265, 1993.
11. Sauvé, R.G., *H3DMAP Version 6 - A General Three-Dimensional Finite Element Computer Code for Linear and Nonlinear Analyses of Structures-User Documentation*, Ontario Hydro Technologies Report No. A-NSG-95-139-P, Dec., 1996.
12. Ho, E. T. C., *Creep, Stress Relaxation and Tensile Testing of Zr-2.5Nb Pressure Tube R912 Material,* Ontario hydro Technologies Report No. A-NFC-96-115-P, Jan. 14, 1997.